[9] Jekeli, C.
Inertial Navigation Systems with Geodetic Applications.
Berlin: Walter de Gruyter, 2000.

[10] Julier, S. J., Uhlmann, J. K., and Durrant-Whyte, H. F.
A new method for the nonlinear transformation of means and covariances in filters and estimators.
IEEE Transactions on Automatic Control, **45**, 3 (Mar. 2000), 477–482.

[11] Lefferts, E. J., Markley, F. L., and Shuster, M. D.
Kalman filtering for spacecraft attitude estimation.
Journal of Guidance, Control, and Dynamics, **5**, 5 (Sept.–Oct. 1982), 417–429.

[12] Markley, F. L.
Attitude error representations for Kalman filtering.
Journal of Guidance, Control, and Dynamics, **26**, 2 (Mar.–Apr. 2003), 311–317.

[13] Rogers, R. M.
Applied Mathematics in Integrated Navigation Systems, (2nd ed.).
Reston, VA: American Institute of Aeronautics and Astronautics, Inc., 2003, ch. 15.

[14] Schaub, H., and Junkins, J. L.
Stereographic orientation parameters for attitude dynamics: A generalization of the Rodrigues parameters.
Journal of the Astronautical Sciences, **44**, 1 (Jan.–Mar. 1996), 1–20.

[15] Shepperd, S. W.
Quaternion from rotation matrix.
Journal of Guidance and Control, **1**, 3 (May–June 1978), 223–224.

[16] Shuster, M. D.
A survey of attitude representations.
Journal of the Astronautical Sciences, **41**, 4 (Oct.–Dec. 1993), 439–517.

[17] van der Merwe, R., Wan, E. A., and Julier, S. I.
Sigma-point Kalman filters for nonlinear estimation and sensor-fusion: Applications to integrated navigation.
Presented at the AIAA Guidance, Navigation and Contol Conference, Providence, RI, Aug. 2004; AIAA-2004-5120.

[18] Wan, E., and van der Merwe, R.
The unscented Kalman filter.
In S. Haykin (Ed.), Kalman Filtering and Neural Networks, New York: Wiley, 2001, ch. 7.

Noncoherent Pulse Compression

Pulse compression can be performed in noncoherent radars by using coded on-off keying (OOK). We show how any bipolar pulse-compression code (e.g., Barker) can be modified into unipolar OOK through Manchester coding. The resulted transmitted signal is a burst of dense subpulses, with pulse position modulation. In the receiver, the envelop-detected signal is aperiodically cross-correlated with a mismatched bipolar reference signal, yielding noncoherent integration with a low-sidelobe response. The concept can be used in simple radars where Doppler information is not required, in direct-detection laser radars and in ultrawideband (UWB) radars. Examples are given with bursts of 13 and 70 subpulses. Detection probabilities dependence on SNR is studied and compared with coherent processing.

I. INTRODUCTION

Coherency provides radar with two major properties: 1) Doppler (range-rate) information on the target, and 2) pulse-compression capability, in which the energy in a modulated, long, low-power pulse, could be integrated through matched filtering, into a virtual short pulse of high power. Over the years a rich library of pulse-compression waveforms has been developed [1, 2]. They are mostly constructed from FM (linear and nonlinear) and phase-coding (bipolar and polyphase).

The suggested noncoherent approach is to break the intended duration of the uncompressed pulse into a burst of dense, noncontiguous subpulses, and use pulse position modulation to implement binary pulse-compression code. The technique can be used in simple radars that do not need Doppler information. It may also be attractive for simple direct-detection laser radars. Indeed, there were already attempts to perform noncoherent integration of a train of optical pulses [3]. The approach there was to dither the pulse position around its nominal value, according to a pseudonoise (PN) code. The signal intensity at the detector was cross-correlated with the known outgoing pulse train. Such cross-correlation between two trains of unipolar pulses yielded many peaks. Due to the

Manuscript received April 14, 2005; revised October 18, 2005; released for publication February 10, 2006.

IEEE Log No. T-AES/42/2/876458.

Refereeing of this contribution was handled by V. C. Chen.

dither, one peak was higher than the rest, representing the true delay. However, the other cross-correlation peaks can cause an erroneous decision, hence an error in the estimated delay. The false peaks of the cross-correlation output play the same role as the sidelobes in the delay response of a conventional coherent radar. We propose here to adapt well-known bipolar pulse-compression waveforms, which yield aperiodic autocorrelation with low sidelobes, to an on-off keying (OOK) type of radar, like laser radar, in order to produce better cross-correlation. The resulted transmitted signal and an appropriate reference signal for cross-correlation processing are described in Section II. The cross-correlation outputs, with and without noise, are demonstrated in Section III, and an example of a longer signal is given in Section IV. An extension to periodic signals is given in Section V. Detection probabilities are obtained in simulations described in the appendix, including comparison with coherent processing.

As far as we know the approach used in [3] is a first description of what is practically a noncoherent pulse compression. Skolnik [4, sect. 11.5] states that "Pulse compression is accomplished by employing frequency or phase modulation to widen the signal bandwidth. (Amplitude modulation is also possible, but is seldom used.)" Only if the sentence in parentheses would have said "Amplitude modulation alone ..." it could be interpreted as a possibility of implementing pulse compression in noncoherent radar. Most likely the quoted statement refers to amplitude modulation in addition to frequency or phase modulation (like in a Huffman signal [2]), which indeed is seldom used.

II. SUGGESTED PULSE-POSITION CODING FOR ON-OFF RADAR PULSES

The procedure for creating a noncoherent pulse-compression system is constituted from the following four steps (each step is demonstrated by the result for a Barker 13 example).

1) Choose a pulse-compression binary sequence.

$$B = \{1\ 1\ 1\ 1\ 1\ 0\ 0\ 1\ 1\ 0\ 1\ 0\ 1\}.$$

2) Create a transmitted sequence T by applying Manchester coding [5] to B. In Manchester coding "1"= 1 0 and "0"= 0 1.

$$T = \{1\ 0\ 1\ 0\ 1\ 0\ 1\ 0\ 1\ 0\ 0\ 1\ 0\ 1\ 1\ 0\ 1\ 0\ 0\ 1\ 1\ 0\ 0\ 1\ 1\ 0\}.$$

Manchester coding is used in OOK optical communication [6]. One of its advantages is that it equates the energy in the original "1" and "0" elements. Note that T represents the actual signal levels, namely when $T = 1$ the signal is on and when $T = 0$ it is off. We refer to such a signal as "unipolar."

3) Create a reference sequence R in which each 0 of T is replaced by -1.

$$R = \{1\ -1\ 1\ -1\ 1\ -1\ 1\ -1\ 1\ -1\ -1\ 1\ -1\ 1\ 1$$
$$-1\ 1\ -1\ -1\ 1\ 1\ -1\ -1\ 1\ 1\ -1\}.$$

When a signal gets the values of R it is referred to as a "bipolar" signal. Using a mismatched bipolar reference signal instead of a unipolar signal, matched to the transmitted signal, will result in a cross-correlation (between T and R) with an average value of zero.

4) Replace each chip of T and R with a narrow pulse of height equal to the chip value, preceded and followed by a null (zero) level. The pulses in the modified T represent the envelope of the transmitted amplitude-modulated carrier (and of the envelope-detected received pulses). Setting a pulsewidth shorter than the chip duration will accommodate radar with limited duty cycle. The pulses in the modified R represent the reference pulses stored in the receiver. Note that the highest output SNR value will be obtained when the widths of the pulses in T and R are equal. In a LIDAR the detected reflected pulses are likely to be wider than the transmitted optical pulses. Hence, the reference pulses should be matched to those wider pulses.

The resulted transmitted (solid line) and reference (dotted line) signals for a Barker 13 case are plotted in Fig. 1. The duty cycle of the transmitted pulses is 1/5. The reference pulses are wider (by a factor of 3) and their magnitude is lower. This was done in order to clarify the plots. The resulted aperiodic cross-correlation is plotted in Fig. 2. The delay scale is normalized with respect to the chip duration of the Barker code.

For comparison Fig. 3 presents the cross-correlation that would have been obtained if the reference signal did not include the negative pulses. The resulted shape resembles the undesired broad trianglular autocorrelation of a long rectangular pulse. The advantage of Fig. 2 over Fig. 3 is obvious. As we show in the next section, the negative reference pulses exhibit some advantages in the presence of noise as well.

III. PROPERTIES OF THE APERIODIC CROSS-CORRELATION OUTPUT

Note in Fig. 2 that except for the two negative near cross-corelation sidelobes, the mainlobe to peak sidelobe ratio is 13 as in a conventional Barker 13 signal. Note also that the overall average of the cross-correlation function is zero. The two negative near-sidelobes (of levels -7 and -6) balance the $+13$ mainlobe. In coherent radar, the carrier phase of the reflected signal can easily change. Hence, a positive decision threshold is applied to the magnitude of the coherent processor's complex output. For this reason, in coherent RF radar, negative cross-correlation

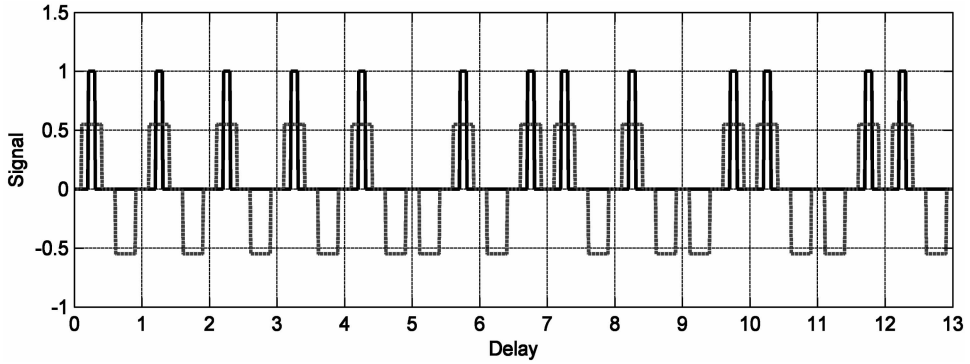

Fig. 1. Transmitted (solid) and reference (dash) signals, based on Manchester-coded Barker 13.

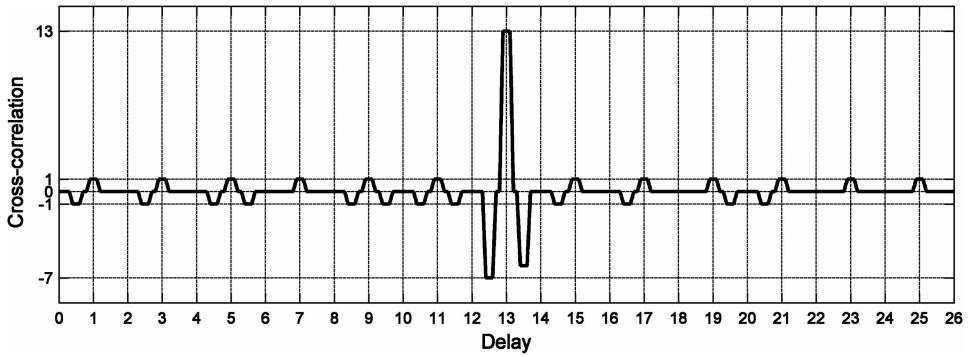

Fig. 2. Cross-correlation between transmitted and reference signals in Fig. 1.

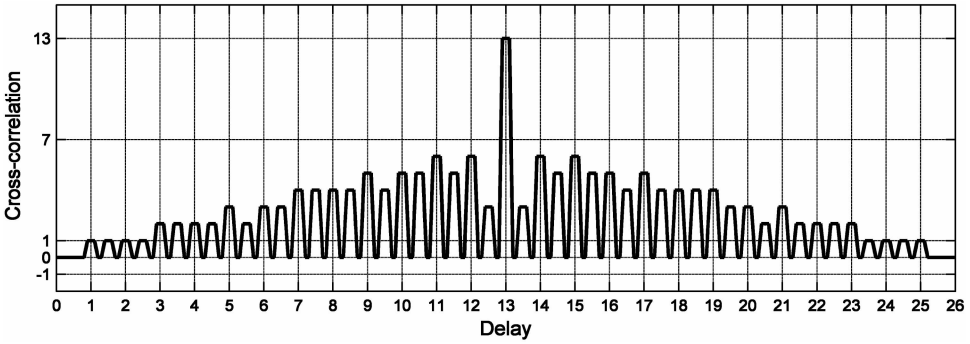

Fig. 3. Cross-correlation when reference signal includes positive pulses only.

sidelobes are as harmful as positive ones. In our case no carrier phase is involved and the cross-correlation cannot be inverted. The mainlobe will always be positive, and therefore the decision threshold will also be set at a positive value. In a coherent radar range, sidelobes can cause two problems: 1) mask the mainlobe of a nearby weaker target, and 2) when noise is added to a large sidelobe it can cause a false threshold crossing. In our noncoherent case, problem 2 is not likely to happen because additive noise is not likely to bring the large negative near-sidelobes all the way to a high positive value, that would cross the threshold. The two large negative sidelobes can still mask a weak second target, but only if the delay difference between the two targets is one chip duration of the transmitted code. If the target reflection is relatively wide, then the correlation output will effectively differentiate the target reflection, emphasizing edges.

The delay resolution of this radar system is approximately equal to the width of the cross-correlation mainlobe. That width is determined by the cross-correlation between a single transmitted subpulse and a single reference subpulse. So the role of the pulse coding is not to improve the delay resolution over that of an individual subpulse, but to allow integration of many dense subpulses without creating ambiguous peaks.

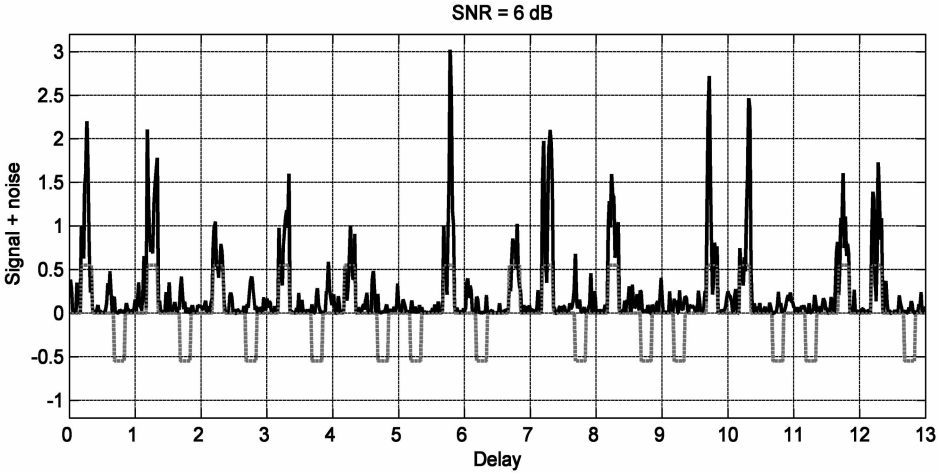

Fig. 4. Envelop detected (solid) signal plus noise, and reference (dash) signal, based on Manchester-coded Barker 13.

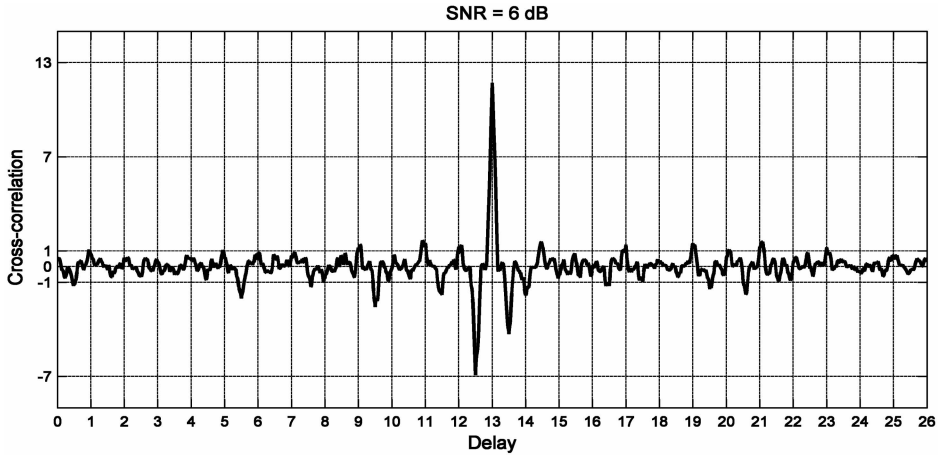

Fig. 5. Cross-correlation between detected and reference signals in Fig. 4.

The added negative reference pulses (which do not exist in the transmitted signal) have a second important role with regard to the noise and clutter output. In coherent radar, adding such unmatched receiving windows will double the output due to clutter and noise power, causing approximately 3 dB SNR loss. In our case, as we show in the appendix, the SNR loss due to the negative reference pulses is typically less than 1 dB. After envelope detection clutter returns and thermal noise are always positive (when not added to a pulse). Because the cross-correlation is performed after envelope detection, adding negative receiving windows, equal in number and area to the positive windows, is expected to reduce the average of the output due only to noise and clutter power. An example of the signal and cross-correlation in the presence of relatively strong noise is shown in Figs. 4 and 5. The envelope detector follows square law. For these plots the width of the reference pulses was made equal to the width of the transmitted pulses (yielding the heighest SNR) and the pulse duty cycle was increased to 1/3. In Fig. 4 we simulated noise bandwidth wider than the inverse of a pulsewidth. There are 10 independent noise samples per pulsewidth, which are filtered using a 3 element sliding window, before being added to the signal. In Fig. 4 the signal plus noise is shown after square-law envelope detection. In the resulted cross-correlation (Fig. 5) we see a tolerable reduction of the mainlobe to peak-sidelobe ratio. Note that without noise the cross-correlation peak in Fig. 5 would be 13 exactly.

The statistics of the peak cross-correlation in the case of noise-only input will determine the probability of false alarm. The statistics of signal plus noise, will determine the probability of detection. Probability density functions (pdfs), obtained from numericall simulations, are presented in the appendix. They are compared with the case where the reference signal includes only the positive pulses. Cross-correlation with a reference signal that contains only the positive pulses is equivalent to performing conventional noncoherent pulse integration. The fact that the transmitted pulses are dense and not equally spaced does not alter that fact.

As the pdfs in the appendix show, the negative pulses of the reference signal change dramatically

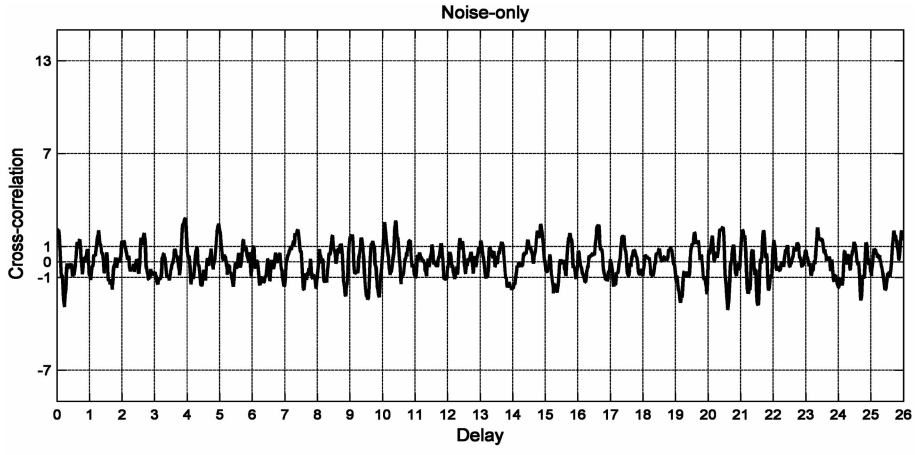

Fig. 6. Cross-correlation with noise-only input. Reference signal includes both positive and negative pulses.

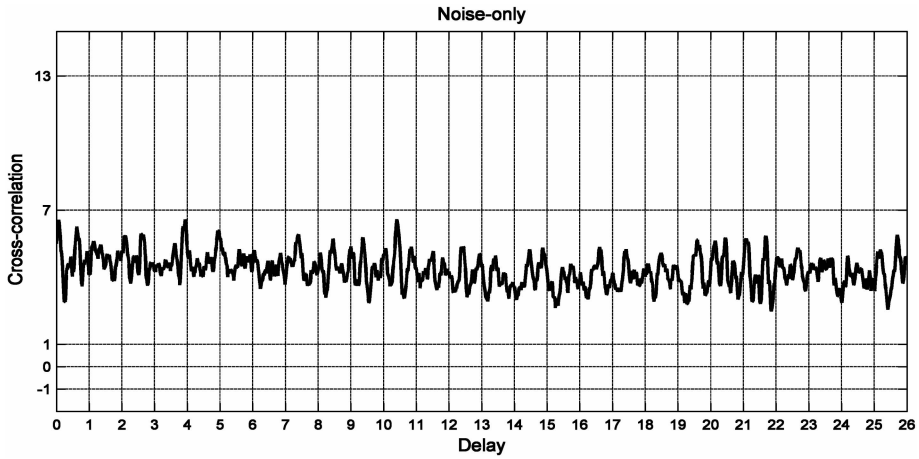

Fig. 7. Cross-correlation with noise-only input. Reference signal includes positive pulses only.

the nature of the output due to noise-only input. A qualitative example of such a case is shown in Figs. 6 and 7. For this noise-only scenario we compare qualitatively the cross-correlation outputs when the reference signal includes the added negative pulses (Fig. 6) and when they are not included (Fig. 7). Comparing Figs. 6 and 7 we see that without the balancing negative pulses of the reference, the cross-correlation output (Fig. 7) has positive values only and reaches a much higher peak. Note that the duration of the noise-only input was not limited to the duration of the reference signal, but was three times longer.

IV. EXAMPLE OF A LONGER CODE

The longest known Barker code is of length 13, which in our case implies that only 13 subpulses are integrated. This may not be very useful. To obtain integration of more subpulses we can resort to longer bipolar pulse-compression codes. In this section we present integration of 70 subpulses, using the longest presently known [7] minimum peak sidelobe (MPSL) binary sequence, with peak sidelobe of 4. The binary sequence is

0 1 1 0 1 0 0 0 0 1 0 0 1 1 0 0 1 1 1 0 1 1 0

1 0 0 1 1 1 0 0 0 1 1 0 0 0 0 1 0 0 1 0 0 1 1

1 1 1 0 1 1 0 1 1 1 0 1 0 1 0 1 0 1 1 1 1 1 1 0.

Following the same procedure as in the Barker 13 case yields the noise-free cross-correlation presented in Fig. 8. The signal duty cycle is 1/3 and the transmitted and reference pulses have the same width. Note that the height of the mainlobe peak is 70 while the peak sidelobe level is 4. The ratio is 17.5, which is better than in the Barker 13 case. The same ratio was obtained in the original MPSL signal of length 70. For other OOK signals based on binary signals we expect the same peak sidelobe ratio as in the corresponding original signals.

V. PERIODIC SIGNALS

So far our noncoherent pulse-compression principle was applied to a single pulse. The coding

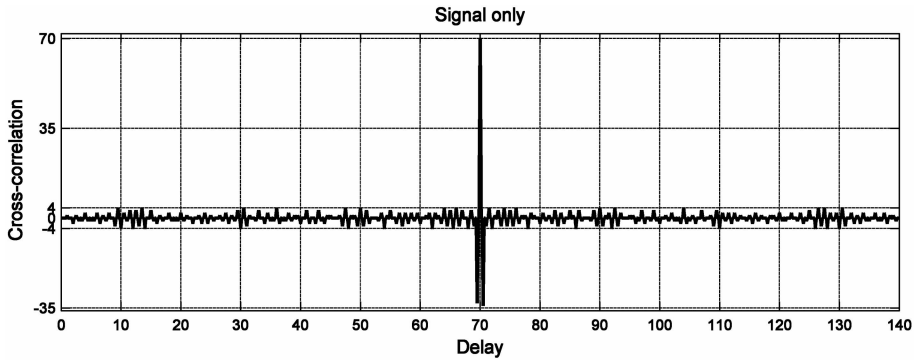

Fig. 8. Cross-correlation between transmitted signal and reference signal, based on MPSL binary code of length 70.

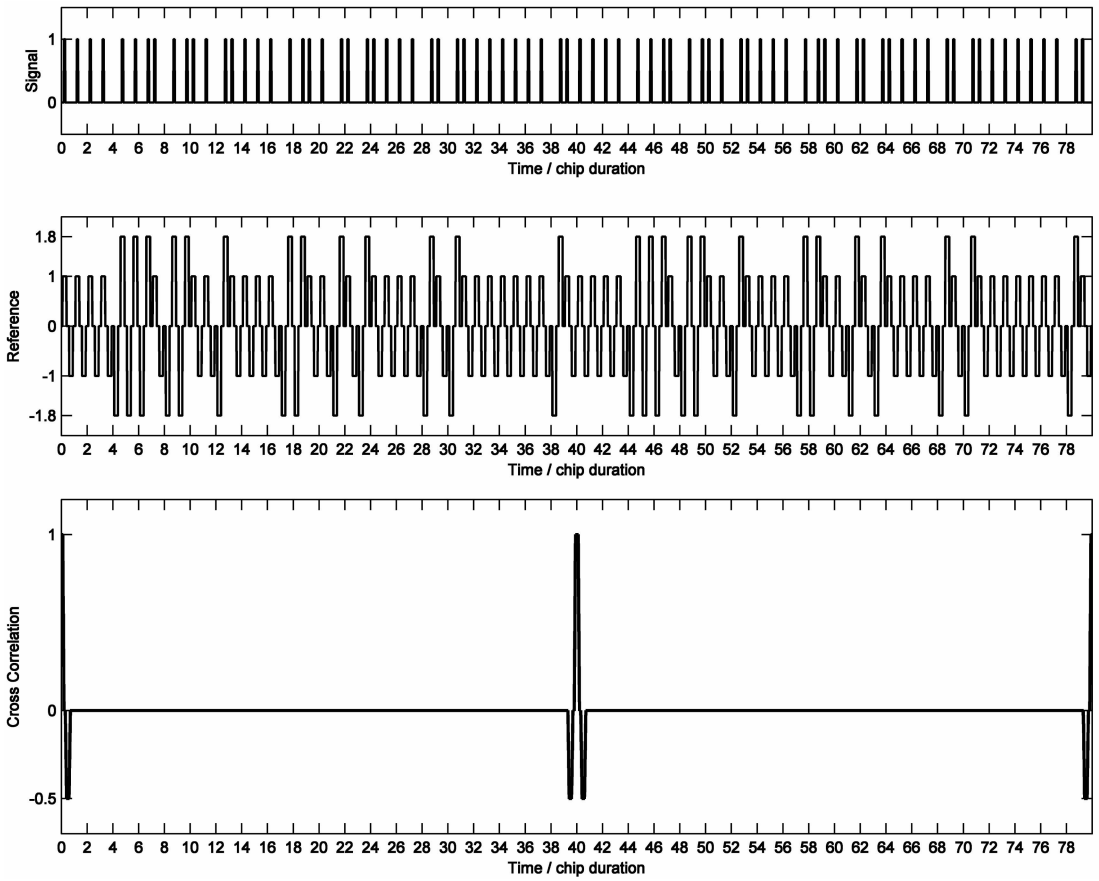

Fig. 9. Transmitted and reference Manchester-coded periodic Ipatov signal, and its periodic cross-correlation. Two periods are shown, each period contains 40 bits.

used in the examples were Barker 13 and MPSL 70. In this section we show that the same principle can be applied to periodic CW signals. Since our scheme converts bipolar keying to OOK, the phrase "continuous wave" is not truly appropriate anymore. However, we will keep referring to them as CW signals because that is how they are referred to in the literature on direct-detection CW lidars with OOK by PN codes [8–11].

Continuing with our approach of modifying well-known bipolar pulse-compression signals, in the CW case we choose to modify what seems to be the most appropriate candidate family of periodic signals—Ipatov's codes [12, 2 (sect. 6.5)]. An Ipatov's signal is transmitted as bipolar signal $\{+1, -1\}$ but the reference signal is mismatched. The resulted periodic cross-correlation is perfect, namely the sidelobes are identically zero. In the Ipatov code $\{1\ 1\ 1\ 1\ 0\ 0\ 0\ 1\ 0\ 0\ 1\ 1\ 0\ 1\ 1\ 1\ 1\ 0\ 0\ 1\ 1\ 0\ 1\ 0\ 1\ 1$ $1\ 1\ 0\ 1\ 0\ 1\ 1\ 1\ 1\ 1\ 1\ 1\ 0\ 1\}$ of length 40, the reference signal is constructed from $\{+1, -1.8\}$.

It is straightforward to apply our Manchester-coded OOK to Ipatov's signals. A demonstration using Ipatov's code of length 40 is given in Fig. 9.

The three subplots show two periods of the periodic transmitted signal (top), the reference signal (middle), and the resulted periodic cross-correlation between the two (bottom). Note that the perfect periodic cross-correlation behavior (zero sidelobes) is maintained except for the two negative near-sidelobes, whose heights are half the height of the mainlobe.

VI. CONCLUSIONS

We showed how to integrate (noncoherently) many dense noncoherent radar pulses by using methods borrowed from coherent radar pulse compression. The delay response of the integrated pulse train maintains a single, narrow, main peak, and very low recurrent peaks. Bipolar pulse-compression codes serve as the basic pulse coding. Manchester coding modifies the bipolar coding and converts the two polarities into two pulse positions. The reference signal, with which the unipolar detected returned pulses are cross-correlated, is not matched. It is a train of both the original positive pulses and an equal number of negative pulses. This kind of mismatched reference signal reduces the recurrent lobes in the presence of the signal it was designed for, yet does not add significant signal-to-noise ratio (SNR) loss (less than 1 dB). Two examples were presented in which the number of integrated pulses were 13 and 70. We also showed that the same concept can be applied to periodic CW signal, and demonstrated it on Ipatov's periodic signal of length 40 that yields near-perfect periodic cross-correlation.

ACKNOWLEDGMENT

The author wishes to thank Mr. Uri Peer who suggested applying the technique to periodic signals.

APPENDIX

The Monte Carlo runs described below were performed in order to study the pdf of the cross-correlation mainlobe, with and without signal, using the two types of reference signals (unipolar and bipolar) designed for the Manchester-coded Barker 13 signal.

The vector of signal samples S was constructed from $M = 13$ identical samples of value A, representing a nonfluctuating target

$$\{S\}_k = A[1\ 1\ 1\ 1\ 1\ 1\ 1\ 1\ 1\ 1\ 1\ 1\ 1]. \tag{1}$$

$N1i$, the first vector of $M = 13$ element noise samples, representing the in-phase component of the noise, was constructed from M independent, identically distributed, random samples from a normal distribution with zero mean and a standard deviation σ specified by the single-pulse SNR,

$$\text{SNR} = \frac{A^2}{2\sigma^2} \Rightarrow \sigma = \frac{A}{\sqrt{2}} 10^{(-\text{SNR dB}/20)} \tag{2}$$

when $A = 1$, SNR of 4 dB implies $\sigma = 0.4462$. This value of σ was used in all the simulations. The value of A and the decision threshold were adjusted for each case, to get a probability of false alarm $P_{\text{FA}} = 0.001$ and a probability of detection $P_{\text{D}} = 0.9895$. Another similar and independent 13 element noise vector $N1q$ was created to represent the quadrature component. Another independent similar pair was also created, labeled $N2i$ and $N2q$.

Following a square-law envelope detector [4], the mainlobe of the cross-correlation with a bipolar reference, when both signal and noise are present, is represented by

$$x = \sum_{k=1}^{M} [(S_k + N1i_k)^2 + N1q_k^2] - \sum_{k=1}^{M} (N2i_k^2 + N2q_k^2). \tag{3}$$

When only noise is present the cross-correlation peak is obtained from

$$x_{\text{noise}} = \sum_{k=1}^{M} (N1i_k^2 + N1q_k^2) - \sum_{k=1}^{M} (N2i_k^2 + N2q_k^2). \tag{4}$$

Histograms of x and x_{noise} obtained with 40000 runs, are plotted in Fig. 10. The histograms were created using $\sigma = 0.4462$. To get the desired probability of false alarm ($P_{\text{FA}} = 0.001$) the threshold was set at 6.45. To get the desired probability of detection ($P_{\text{D}} = 0.9895$) required $A = 1.0752$, implying a single-pulse SNR of 4.63 dB. The histograms were plotted using MATLAB's **ksdensity** function with the Epanechnikov kernel. The **ksdensity** function produces a nonparametric density estimate using a kernel smoothing technique.

When the reference signal contains only positive pulses, the mainlobe of the cross-correlation corresponds to conventional noncoherent integration of M pulses, following a square-law detector. The signal-plus-noise case is given by

$$y = \sum_{k=1}^{M} [(S_k + N1i_k)^2 + N1q_k^2]. \tag{5}$$

The noise-only case is represented by

$$y_{\text{noise}} = \sum_{k=1}^{M} (N1i_k^2 + N1q_k^2). \tag{6}$$

The corresponding histograms are plotted in Fig. 11. The histograms were created using $\sigma = 0.4467$. To

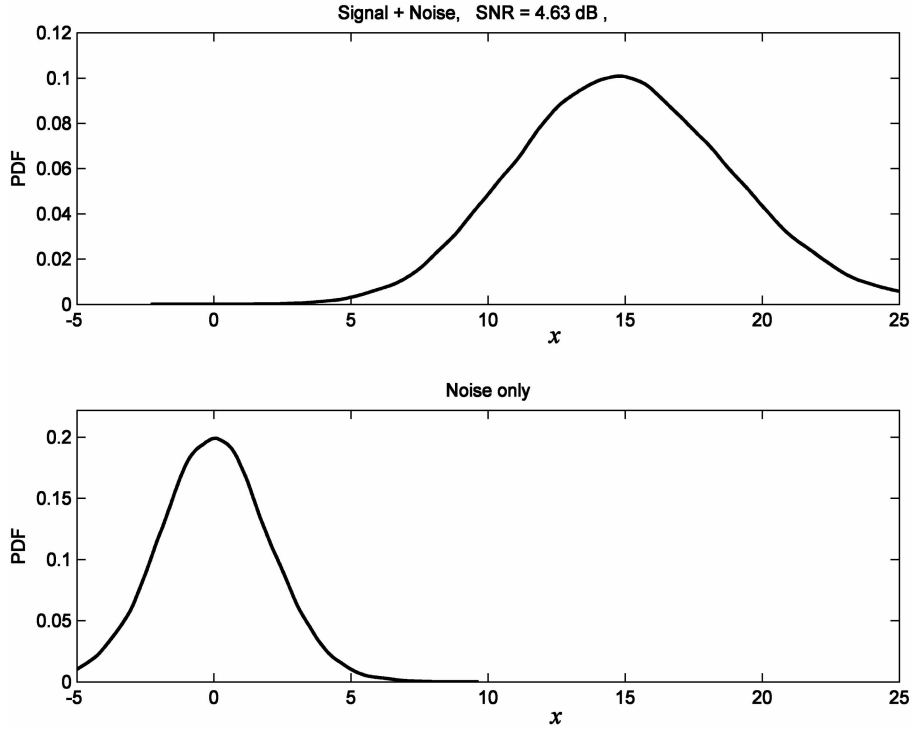

Fig. 10. PDFs corresponding to correlation with bipolar reference. Top: signal + noise. Bottom: noise only.

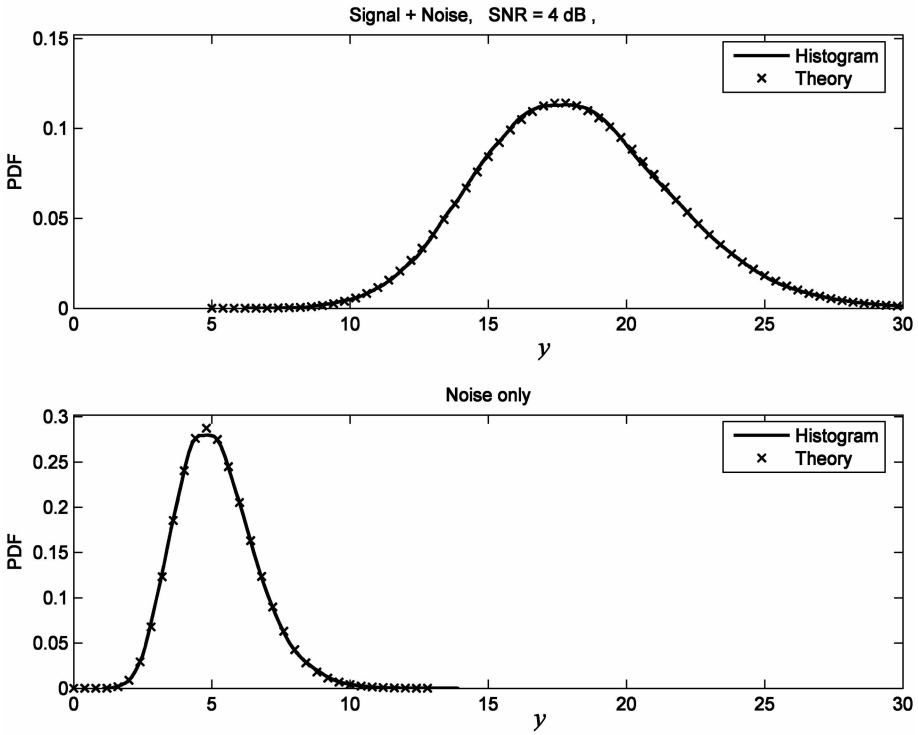

Fig. 11. PDFs corresponding to correlation with unipolar reference. Top: signal + noise. Bottom: noise only.

get $P_{\mathrm{FA}} = 0.001$ the threshold was set at 10.95. To get $P_{\mathrm{D}} = 0.9895$ required $A = 1.0$, implying a single-pulse SNR of 4 dB. The histograms in Fig. 11 represent the pdfs of conventional noncoherent integration of 13 pulses reflected from a nonfluctuating target (Swerling 0) and detected by a square-law envelope detector. The theoretical density functions, with and without signal are given by

$$p(y) = \frac{1}{2\sigma^2(M-1)!}\left(\frac{y}{MA^2}\right)^{(M-1)/2} \times \exp\left(\frac{-y-MA^2}{2\sigma^2}\right) \mathrm{I}_{M-1}\left(\frac{A}{\sigma^2}\sqrt{My}\right) \quad (7)$$

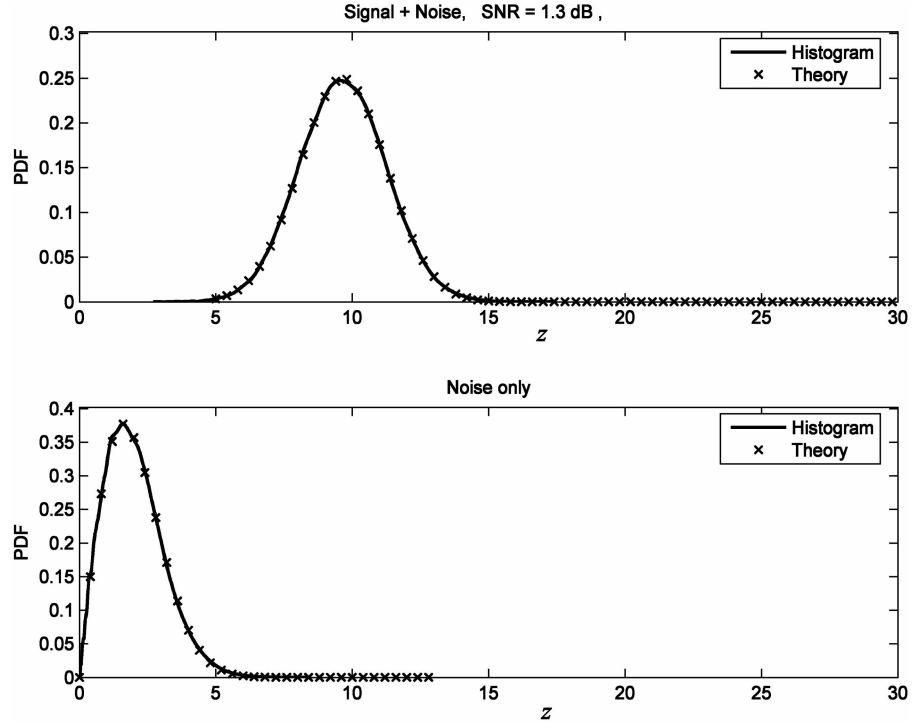

Fig. 12. PDFs corresponding to coherent integration. Top: signal + noise. Bottom: noise only.

$$p(y \mid A=0)=\frac{1}{2\sigma^2(M-1)!}\left(\frac{y}{2\sigma^2}\right)^{M-1}\exp\left(\frac{-y}{2\sigma^2}\right). \tag{8}$$

The theoretical pdfs are plotted in Fig. 11, on top of the corresponding histogram results, showing excellent agreement, thus validating the simulation. The corresponding theoretical SNR required for the specified P_{D} and P_{FA} is 3.94 dB, calculated using the Shnidman approximation [13].

The detection performance of coherently detected Barker 13 signal is obtained by treating the Barker signal as coherent integration of $M = 13$ pulses. The signal-plus-noise case is represented by

$$z=\sqrt{\left[\sum_{k=1}^{M}(S_k+N1i_k)\right]^2+\left(\sum_{k=1}^{M}N1q_k\right)^2} \tag{9}$$

and the noise-only case by

$$z_{\mathrm{noise}}=\sqrt{\left(\sum_{k=1}^{M}N1i_k\right)^2+\left(\sum_{k=1}^{M}N1q_k\right)^2}. \tag{10}$$

The histograms in Fig. 12 represent the pdfs of the coherent integration output z. In order to get the required $P_{\mathrm{FA}} = 0.001$ the threshold for the coherent processing had to be set at 5.98. The required $P_{\mathrm{D}} = 0.9895$ was obtained with $A = 0.7328$ implying a single-pulse SNR of 1.3 dB. The theoretical pdfs for this form of coherent integration are given by

$$p(z)=\frac{z}{M\sigma^2}\exp\left(\frac{-z^2-M^2A^2}{2M\sigma^2}\right)\mathrm{I}_0\left(\frac{Az}{\sigma^2}\right) \tag{11}$$

$$p(z \mid A=0)=\frac{z}{M\sigma^2}\exp\left(\frac{-z^2}{2M\sigma^2}\right). \tag{12}$$

The theoretical pdfs are plotted in Fig. 12, on top of the corresponding histogram results, again showing excellent agreement. The corresponding theoretical SNR required for the specified P_{D} and P_{FA} is 1.26 dB.

A summary of the detection performances appears in Table I. We can conclude that: 1) noncoherent processing caused an SNR loss of 2.7 dB, and 2) adding the negative reference pulses caused an additional loss of only 0.63 dB. Recall that adding the negative reference pulses is what mitigated the sidelobes of the aperiodic cross-correlation.

TABLE I
Detection Performances of 13 Subpulses

Processing	Coherent	Noncoherent, Unipolar Reference	Noncoherent, Bipolar Reference
P_{FA}	0.001	0.001	0.001
P_{D}	0.9895	0.9895	0.9895
Single subpulse SNR [dB]	1.3	4	4.63
Theoretical SNR [dB]	1.26	3.94	—
Loss [dB]	0	2.7	2.7 + 0.63 = 3.33

The excellent agreement with theoretical results, of the required SNR obtained from the simulations in the matched unipolar case, and in the coherent processing case, testifies to the validity of the simulations. We can therefore assume that the simulation results obtained with the new mismatched bipolar reference are also valid, and the conclusion that the mismatch processing caused an additional SNR loss of only 0.63 dB (for the code based on Barker 13) is correct.

Nadav Levanon
Dept. of Electrical Engineering Systems
Tel Aviv University
PO Box 39040
Tel Aviv 69978
Israel

REFERENCES

[1] Cook, C. E., and Bernfeld, M.
Radar Signals: An Introduction to Theory and Application.
New York: Academic Press, 1967.

[2] Levanon, N., and Mozeson, E.
Radar Signals.
New York: Wiley, 2004.

[3] Peterson, R. D., and Schepler, K. L.
Timing modulation of a 40-MHz laser-pulse train for target ranging and identification.
Applied Optics, **42**, 36 (2003), 7191–7196.

[4] Skolnik, M. I.
Introduction to Radar Systems (2nd ed.).
New York: McGraw Hill, 1980.

[5] Stremler, F. G.
Introduction to Communication Systems (2nd ed.).
Reading, MA: Addison-Wesley, 1982, sec. 7.6.

[6] Jau, L. L., and Lee, Y. H.
Optical code-division multiplexing systems using Manchester coded Walsh codes.
IEE Proceedings on Optoelectronics, **151**, 2 (2004), 81–86.

[7] Coxson, G., and Russo, J.
Efficient exhaustive search for optimal-peak-sidelobe binary codes.
IEEE Transactions on Aerospace and Electronic Systems, **41**, 1 (2005), 302–308.

[8] Takeuchi, N., Sugimoto, N., Baba, H., and Sakurai, K.
Random modulation CW lidar.
Applied Optics, **22**, 9 (1983), 1382–1386.

[9] Nagasawa, C., Abo, M., Yamamoto, H., and Uchino, O.
Random modulation CW lidar using new random sequences.
Applied Optics, **29**, 10 (1990), 1466–1470.

[10] Emery, Y., and Flesia, C.
Use of the A1- and the A2-sequences to modulate continuous-wave pseudorandom noise lidar.
Applied Optics, **37**, 12 (1998), 2238–2241.

[11] Rybaltowski, A., and Taflove, A.
Suprior signal-to-noise ratio of new AA1 sequence for random-modulation continuous-wave lidar.
Optics Letters, **29**, 15 (2004), 1709–1711.

[12] Ipatov, V. P.
Periodic discrete signals with optimal correlation properties.
Radio I Svyaz , Moscow, (1992). English translation, the University of Adelaide, Australia, ISBN 5-256-00986-9.

[13] Shnidman, D. A.
Determination of required SNR values.
IEEE Transactions on Aerospace and Electronic Systems, **38**, 3 (2002), 1059–1064.